Improved analysis of SN1987A antineutrino events

G. Pagliaroli, F. Vissani, M.L. Costantini, A. Ianni

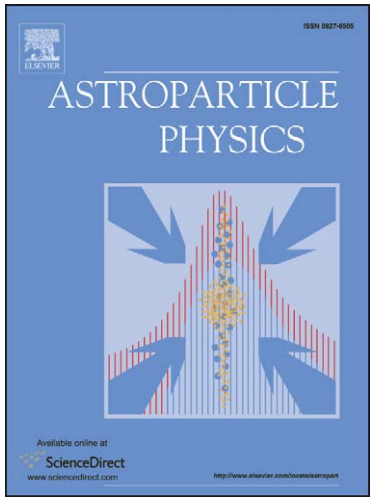

Improved analysis of SN1987A antineutrino events

G. Pagliaroli, F. Vissani, M.L. Costantini, A. Ianni

PII: S0927-6505(08)00196-5
DOI: 10.1016/j.astropartphys.2008.12.010
Reference: ASTPHY 1372

To appear in: *Astroparticle Physics*

Received Date: 5 November 2008
Revised Date: 17 December 2008
Accepted Date: 24 December 2008

Please cite this article as: G. Pagliaroli, F. Vissani, M.L. Costantini, A. Ianni, Improved analysis of SN1987A antineutrino events, *Astroparticle Physics* (2009), doi: 10.1016/j.astropartphys.2008.12.010

Improved analysis of SN1987A antineutrino events

G. Pagliaroli,[1,2,*] F. Vissani,[1,†] M. L. Costantini,[1,2,‡] and A. Ianni[1,§]

[1] *INFN, Laboratori Nazionali del Gran Sasso, Assergi (AQ), Italy*
[2] *University of L'Aquila, Coppito (AQ), Italy*

(Dated: December 17, 2008)

We propose a new parameterization of the antineutrino flux from core collapse supernovae, that allows an interpretation of its astrophysical parameters within the Bethe and Wilson scenario for the explosion, and that leads to a reasonable (smooth) behavior of the average energy and of the luminosity curve. We apply it to analyze the events observed by Kamiokande-II, IMB and Baksan detectors in correlation with SN1987A. For the first time, we consider in the same analysis all data characteristics: times, energies and angles of the observed events. We account for the presence of background and evaluate the impact of neutrino oscillations. The hypothesis that the initial luminous phase of emission (accretion) is absent can be rejected at the 2% significance level. Without the need to impose external priors in the likelihood analysis, the best-fit values of the astrophysical parameters are found to be in remarkable agreement with the expectations of the standard core-collapse scenario; in particular, the electron antineutrino-sphere radius is 16 km, the duration of the accretion phase is found to be 0.55 s, and the initial accreting mass is 0.22 $M_\odot$. Similarly the total energy emitted in neutrinos is 2.2×10^{53} erg, again close to the expectations. The errors on the parameters are evaluated and found to be relatively large, consistently with the limited number of detected events; the two dimensional confidence regions, that demonstrate the main correlations between the parameters, are also given.

PACS numbers: 97.60.Bw Supernovae; 26.30.Jk Weak interaction and neutrino induced processes; 95.55.Vj Neutrino detectors; 14.60.Pq Neutrino mass and mixing.

I. INTRODUCTION

We begin recalling the interest of core collapse supernovae, the status of their understanding, and the expectations for neutrino emission in the standard scenario. Next, we discuss in Sect. I B the motivations for an improved analysis of SN1987A observations in the context of the standard scenario, collecting remarks and caveats in Sect. I C. Finally, we offer in Sect. I D the outline of the present investigation.

A. Neutrino emission in core collapse supernovae

Core collapse supernovae (SN) are astrophysical events in which all known forces interplay with each other in extreme physical conditions. An adequate modeling of the processes occurring during this event would be important to obtain information on the left-over compact star [1], on nucleosynthesis [2–4], on the properties of the supernova remnant [5], and on the expected signals during the explosion; in particular, gravitational waves and neutrinos [6, 7].

Because of the complexity of the problem, the modeling of the physical processes is still in evolution, but it is generally accepted that the role of neutrinos is critical for the energy transport as first suggested in [8]. The collapse and the formation of a compact object, like a neutron star, have to pass through substantial neutrino emission, see, e.g., [9]. The details of how the explosion takes place and how the neutrinos are emitted are less clear and necessarily model dependent. In this work we focus on the only mechanism that has been studied in some detail: the *neutrino-driven mechanism* also known as Bethe and Wilson scenario [10] or delayed scenario for the explosion. In the neutrino-driven mechanism, the explosion of the massive star receives crucial assistance from the energy deposition due to an initial, intense neutrino luminosity. Although the viability of this mechanism cannot be considered fully demonstrated at present[1], recent theoretical results [12, 13] encourage the opinion that the neutrino-driven mechanism works for certain core collapse SN.

In the neutrino-driven mechanism, there are two main phases of neutrino emission:
i) A thermal phase, called *cooling*, occurring when the proto-neutron star cools quietly. This phase involves most of the emitted neutrinos, 80-90% in energy.
ii) A brief and very luminous neutrino emission, here termed *accretion*, that should involve a lower amount of neutrinos, 10-20% in energy. The accretion phase characterizes the neutrino-driven mechanism of the explosion, and it is expected to occur in the first stage of neutrino emission. In this phase, the matter is rapidly accreting

*Electronic address: giulia.pagliaroli@lngs.infn.it
†Electronic address: francesco.vissani@lngs.infn.it
‡Electronic address: marialaura.costantini@lngs.infn.it
§Electronic address: aldo.ianni@lngs.infn.it

[1] We note that relevant discussion can be traced back to 1978 with the calculations of Nadyozhin [11].

over the proto-neutron star through the stalled supernova shock wave. The two most important processes of neutrino emission are

$$e^- \; p \rightarrow n \; \nu_e \text{ and } e^+ \; n \rightarrow p \; \bar{\nu}_e \tag{1}$$

due to the abundant presence of nucleons and of quasi-thermal e^+e^- plasma. These types of neutrinos (ν_e and $\bar{\nu}_e$) transfer to the star a small fraction of their energy, $f \sim 0.1$, necessary to revive the stalled shock wave. See [14] for a wide description of the phase of accretion, enriched by analytical arguments.

The neutrinos from phases *i*) and *ii*) can be observed in conventional supernova neutrino detectors (namely, water Cherenkov and scintillators). In particular electron antineutrinos give signal mainly through inverse beta decay reaction on free protons:

$$\bar{\nu}_e \; p \rightarrow e^+ \; n \tag{2}$$

Thus the existence of the accretion and cooling phases, generically expected in the neutrino-driven scenario, can be experimentally verified.

Before proceeding, we recall the existence of a very luminous but much briefer emission phase called *neutronization* that precedes the previous two phases. Although well characterized in time and in flavor (only ν_e are emitted), this phase is expected to involve only $\sim 1\%$ of the energy thus leading to a very small number of events in the standard scenario. This is the reason why we will disregard it in the following discussion.

B. What can we learn from SN1987A observations?

SN1987A is the first and the only occasion at present to test the credibility of the various hypotheses on how a SN works. In fact, the events observed by IMB [15, 16], Kamiokande-II [17, 18] and Baksan [19], represent a historic opportunity to investigate the physics of the collapse and of the explosion. A very extensive literature testifies the effort to extract information from these data with a wide variety of methods [20–43]. Usually, a specific characteristic of the SN1987A data is studied, most frequently the energy distribution. The energy and the time distributions are jointly considered in a few analyses, but most often describing the neutrino emission with (overly) simple models, a procedure that is only partially justified by the limited amount of events collected.

The next neutrino observation will be an extraordinary occasion to progress, suffice it to recall the existence of the SuperNova Early Warning System (SNEWS) [44] that integrates the observation of many detectors. But we also recall that SN are rare on human time scale and it is not possible to reliably predict when the next one will happen. Thus, we should try our best using the only data that we have at our disposal, and in particular, we should attempt to address the question on *whether there is a hint of accretion from SN1987A observations*, as expected. In this respect, a point that deserves to be stressed is that all detectors observed a relatively large number of events in the first second of data taking, about 40 %: there are in fact 6 events in Kamiokande-II, 3 events in IMB and 2 events in Baksan.

A milestone for the point of discussion and more in general for SN1987A data analysis is the paper of Lamb and Loredo [35] (LL in the following), where it is argued that the SN1987A observations can be used to claim for an evidence of the accretion phase. The LL paper, widely cited in theoretical and experimental reviews, is generally considered a useful application of refined statistical techniques and, in the present paper, we will provide the first independent verification of their results. However, we deem that, in view of the importance of their claim and in the light of various advances in neutrino physics (e.g., in oscillations, [45–48] and [49–56]), it is necessary to offer a critical discussion of the assumptions of the analysis by Lamb and Loredo. More specifically:
1) the likelihood structure can be enhanced including a more accurate detection cross section [57], the information on the directions of the events, a different treatment of the background [43], and a treatment of the efficiency of detection that follows from its definition, as described in Appendix A;
2) the parameterization of the neutrino emission, necessary for the analysis of data, can be improved and can be rendered much more similar to what we expect from the numerical simulations and oscillations have to be included, as discussed in Sect. III and Appendix B. In this respect, a specific criticism was raised by Raffelt and Mirizzi [41], who emphasized that the two-phase parameterization used in LL analysis leads to a sudden jump of the average neutrino energy while passing from accretion to cooling. This behavior is rather different from the expectations of the numerical simulations.

In short, our main tasks are to present a somewhat different likelihood, to propose an improved parameterization for neutrino flux, to include oscillations, and finally to evaluate the impact of the various new points for the analysis of SN1987A observations.

C. LSD events and non standard collapses

Before entering the calculations, it is important to recall that 5 more events have been seen in the Mont Blanc (LSD) detector 4.7 hours before the other events [58]. They cannot be associated with those seen by IMB, Kamiokande-II and Baksan at least in the context of the standard scenario for neutrino emission described above.

These events lead several authors to speculate on the possibility of major deviations from the standard picture of the explosion and of the neutrino emission. Multiple neutrino emission scenarios have been proposed, where the LSD events correspond to the first emission and consist of very low energy electron antineutrinos [59] or alternatively of energetic electron neutrinos [60], that can

be missed by the other detectors. The implementation of the first possibility requires a very (exceedingly) large amount of energy, whereas the second one seems more plausible from the astrophysical point of view. However, even the second possibility seems to be insufficiently elaborated to explain also the events seen by IMB, Kamiokande-II and Baksan; for a recent attempt in this direction, see [61].

In the present paper, we do not attempt an interpretation of the events seen by Mont Blanc. However, the results of our analysis may be regarded as valuable constraint on the last emission of a hypothetical multiple neutrino emission scenario.

D. Layout of the work

The structure of this paper is the following: in Sect. II we discuss the construction of the likelihood function involved in the analysis of the data set, underlining the improvements carried in the description of detection rate; in Sect. III we propose a new parameterization for neutrino emission, building it step by step and discussing its features, leaving the description of certain technical details to Appendices A and B; finally in Sect. IV we draw the results of our analysis.

II. LIKELIHOOD CONSTRUCTION

In this section we describe the likelihood that we adopted to compare the observed events and the assumed flux for the neutrino emission, stressing the novelties and the technical improvements.

A. Signal rate

The signal in each detector, triply differential in time, positron energy E_e and cosine of the angle θ between the antineutrino and the positron is:

$$R(t, E_e, \cos\theta) = N_p \frac{d\sigma_{\bar\nu_e p}}{d\cos\theta}(E_\nu, \cos\theta)\ \Phi_{\bar\nu_e}(t, E_\nu) \times \times \xi_d(\cos\theta)\ \eta_d(E_e)\ \frac{dE_\nu}{dE_e}, \quad (3)$$

where N_p is the number of targets (=free protons) in the detectors, $\sigma_{\bar\nu_e p}$ is the inverse beta decay cross section (Eq. 2), η_d the–detector dependent–average detection efficiency, ξ_d is the angular bias =1 for Kamiokande-II and Baksan whereas for IMB $\xi_d(\cos\theta) = 1 + 0.1\cos\theta$ [16], and, finally, $\Phi_{\bar\nu_e}$ is the electron antineutrino flux, differential in the antineutrino energy E_ν and discussed later in this work.

The expected number of signal events is the crucial ingredient, along with the expected number of background events, to construct the likelihood. To evaluate it we use Eq. 3. The number of expected signals in a bin is just

$$R(t, E_e, \cos\theta) dt dE_e d\cos\theta \quad (4)$$

so that the total number of the events is just the integral of $R(t, E_e, \cos\theta)$ over its three variables.

As mentioned in the introduction, our analysis is similar to the one of Lamb and Loredo [35], with whom we agree when we strictly stick to their procedure. The signal rate that we adopted in this paper departs from their one in the following two points:

1. *Cross section and event direction*

We adopt the inverse beta decay cross section calculated in [57] and in particular we use the differential expression $d\sigma_{\bar\nu_e p}/d\cos\theta$ given in Eq. (20) of that paper. The energy of antineutrino is given in terms of the positron energy E_e and of the angle θ between the antineutrino and the positron directions:

$$E_\nu = \frac{E_e + \delta_-}{1 - (E_e - p_e\cos\theta)/m_p}, \quad (5)$$

where $\delta_- = (m_n^2 - m_p^2 - m_e^2)/(2m_p) = 1.294$ MeV and p_e is the positron momentum. The new total cross section agrees at 10 MeV with the one used by Lamb and Loredo, whereas at 20 MeV (30 MeV) it is 6% (12%) smaller.

2. *Efficiency*

We include in Eq. 3 the detection efficiency as a function of the true energy of the event. This treatment of the efficiency is a straightforward extension of the treatment described in Ref. [32], the one adopted in the most recent analyses of SN1987A data [41, 42]. A different treatment of the efficiency has been advocated in [35]; we will discuss the impact of this treatment on the analysis of SN1987A data in Sect. IV A. A formal justification of our procedure is given in Appendix A, that is based on Ref. [62]. Further discussion is provided in the following of this section.

The efficiency simply accounts for the fact that the expected number of *signal* events should include all relevant detector dependent features: loss of events due to light attenuation, fluctuations of the number of photoelectrons, detector geometry, *etc.*. These features produce an imperfect ($\eta_d < 100\%$) detection efficiency, that means that only a fraction of the produced positrons is actually detected. We have in mind an *average efficiency* evaluated by a MC procedure, namely 1) simulating several events with true energy E_e but located in the various positions and emitted in all possible directions, then 2) counting the fraction of times that an event is recorded, finally 3) deducing also the 'smearing', namely,

the average error as a function of E_e. (Compare also with Eq. A11.)

We recall that for an even more refined analysis of the data, one should not use the average detection efficiency, but should rather evaluate the specific detection efficiency and background rate for any individual event. In our understanding, a correction on individual basis of this type was performed only to assess the errors on the energies of the events, see [18]. (Compare also with Eq. 9 below).

B. The assumed likelihood

We define the following χ^2:

$$\chi^2 \equiv -2 \sum_{d=k,i,b} \log(\mathcal{L}_d), \tag{6}$$

where $\mathcal{L}_d$ is the likelihood of any detector (k, i, b are shorthands for Kamiokande-II, IMB, Baksan). We will use it to estimate the parameters of the emission model and to compare various models, keeping into account the different number of model parameters. For these applications, we will not need the absolute value of the χ^2–i.e., the absolute normalization of the likelihood–but only the differences of χ^2 values–i.e., the various likelihood ratios. Incidentally, we stress that the χ^2 in Eq. 6 permits to handle the likelihood in a numerically convenient way.

We use Poisson statistics to evaluate the likelihoods. For each of the 3 detectors, the likelihood is assumed to be:

$$\begin{aligned} \mathcal{L}_d = e^{-f_d \int R(t)dt} \times \textstyle\prod_{i=1}^{N_d} e^{R(t_i)\tau_d} \times \\ \times \left[\frac{B_i}{2} + \int R(t_i, E_e, \cos\theta_i) G(E_e, E_i) dE_e \right]. \end{aligned} \tag{7}$$

This equation is the basic statistic tool that we will use; we sketch in Appendix A the derivation of its main features and discuss it in detail in the present section. Let us begin by clarifying the notations. We denote by $R(t)$ the integral of $R(t, E_e, \cos\theta)$ over the variables E_e and $\cos\theta$. f_d is the live-time fraction of the detector and τ_d is the dead-time. Each detector saw N_d events; their time, energy and cosine with supernova direction are called t_i, E_i and c_i ($i = 1...N_d$). The precise meaning of t_i, of the smearing function G and of the background rate B_i will be explained in Sect. II B 1, II B 2 and II B 3 respectively.

The previous equation corresponds to Eq. A16, suitably generalized to take into account the dependence of the signal and of the background from the positron direction (see Sect. II A 1 and II B 3). Furthermore, we omitted from Eq. A16 the bin sizes $\delta t \delta E$ and the constant factor $\exp(-\int_T B)$, that contribute only to the normalization of the likelihood and are thus irrelevant for the statistical analysis. Finally, we note that, strictly speaking, Eq. 7 corresponds to Eq. A16 in the limit $f_d \to 1$ and $\tau_d = 0$, that is appropriate for Kamiokande-II and Baksan but not for IMB. Following [31], we took into account the specific features of the IMB detector by introducing a finite dead-time τ_d after each detected events and a live-time fraction $f_d < 1$ (mostly due to the muons). We replaced the numerical value $f_d = 0.8/6 \approx 0.87$ with the value recommended in [35] although this change is not very important. In summary, for IMB, the live-time fraction is $f_d = 0.9055$ and the dead-time is $\tau_d = 0.035$ s, whereas for the other detectors, $f_d = 1$ and $\tau_d = 0$.

1. Absolute and relative times

The absolute times have not been measured precisely enough (except for IMB). Our procedure of analysis however requires only the relative times between the events, the experimental input being $\delta t_i = t_i^{\rm exp} - t_1^{\rm exp}$. The times t_i are defined as follows:

$$t_i = t^{\rm off} + \delta t_i \tag{8}$$

where $t^{\rm off} \geq 0$ is the offset (or delay) time between the first neutrino that reached the Earth (that, by definition, occurred at $t = 0$) and the first event that was detected. We introduce one parameter $t^{\rm off}$ for each detector, and fit their values from the data. The integral over the time in the first exponential factor of Eq. 7 is performed from the moment when the first neutrino reaches the Earth till the end of data taking, $t = 30$ s; the condition that all the data are included imposes mild restrictions, such as $t^{\rm off}_{\rm KII} < 6$ s, that do not have a relevant role in the analysis.

2. Errors

Let us discuss the treatment of the errors in Eq. 7. G is a Gaussian distribution that includes the estimated values of the energy E_i and the error of the energy δE_i for each individual event, accounting for the detector-dependent effects on energy measurements:

$$G(E, E_i) = \frac{1}{\sqrt{2\pi}\delta E_i} e^{-\frac{(E-E_i)^2}{2\ \delta E_i^2}} \tag{9}$$

The inclusion of the error on the measurement of $\cos\theta$ does not change significantly the likelihood, so we simply set $\cos\theta = c_i$ for each event. [For the first 12 Kamiokande-II and for the 8 IMB events the value of $\cos\theta = c_i$ is measured; we set instead $c_i = 0$ for the 5 events of Baksan and the last 4 events out of 16 of Kamiokande-II]. Finally, we do not describe or include the error on the event times δt_i, since the relative time of each event is precisely measured.

3. Background

The probability that an event is due to background is denoted by B_i in Eq. 7. It is calculated as $B_i = B(E_i)$:

it is the *measured* background rate for the given energy [Hz/MeV]. The background distribution differential in time, energy and cosine is $B(E_e)/2$; the factor 1/2 describes a uniform cosine distribution. This definition is different from the one of LL, $B_i = \int B(E_e)\mathcal{L}_i(E_e)dE_e$, that has been argued to be inaccurate in [43].
The values of B_i that we use for Kamiokande-II are given in Appendix A of [43]. The events of Kamiokande below 7 MeV have a higher background rate than found by LL, those above 9 MeV a lower background rate, while the other ones stay almost unchanged.
The changes for Baksan are instead negligible.
It is fair to assume in good approximation that, in the time window of interest, IMB observations are safe against background contamination.

III. ANTINEUTRINO FLUX DESCRIPTION

In this section we describe the parameterization of the neutrino flux that we adopt. We describe the signal introducing three 'microscopic' (i.e., physically meaningful) parameters for each phase, that, roughly speaking, are needed to quantify the duration of the emission process, the intensity of the emission and the average energy of the antineutrinos. The adopted time distributions are constructed to enforce the continuity of the instantaneous luminosity and of the average energy as found in the numerical simulations. Moreover, we tried to maintain the parameterization as simple as possible.

A. Parameterized antineutrino fluxes

1. Cooling phase

In the last phase of the SN collapse the nascent proto-neutron star evolves in a hot neutron star (with radius R_{ns}) and this process is characterized by a neutrinos and antineutrinos flux of all species. This is the *cooling* phase; we use the suffix c in the corresponding symbols.

A rather conventional parameterization of the electron antineutrino flux, differential in the energy is:

$$\Phi_c^0(t, E_\nu) = \frac{1}{4\pi D^2}\frac{\pi c}{(hc)^3} \times 4\pi R_c^2 \; g_{\bar{\nu}_e}(E_\nu, T_c(t)) \quad (10)$$

where the Fermi-Dirac spectrum of the antineutrinos is

$$g_{\bar{\nu}_e}(E_\nu, T_c(t)) = \frac{E_\nu^2}{1 + \exp[E_\nu/T_c(t)]} \quad (11)$$

The time scale of the process is included in the function:

$$T_c(t) = T_c \exp[-t/(4\tau_c)]. \quad (12)$$

Eq. 10 describes an isotropic emission of antineutrinos from a distance $D(= 50$ kpc in the case of SN1987A). [We use the symbol Φ^0 rather than Φ to emphasize that flavor oscillations have not been included yet].

The astrophysical free parameters are R_c, T_c, and τ_c namely: the radius of the emitting region (neutrino sphere), the initial temperature, and the time constant of the process. We recall which are the generic expectations: $R_c \sim R_{ns} = 10 - 20$ km, $T_c = 3 - 6$ MeV, and $\tau_c =$few-many seconds. Rather than using these *a priori*, we will deduce the value of these parameters by fitting the SN1987A data, and later, we will compare the results with the expectations.

2. Accretion phase

After the bounce, the simulations indicate that the shock wave, propagating into the outer core of the star, looses energy and eventually gets stalled. It forms an accreting shock that encloses a region of dissociated matter and hot e^+e^- plasma, where the weak reactions of Eq. 1 give rise to intense ν_e and $\bar{\nu}_e$ luminosities. This emission lasts a fraction of a second. In Appendix B we describe in more details the conceptual scheme for $\bar{\nu}_e$ emission: a neutron target exposed to a flux of thermal positrons. The neutrons are treated as a transparent target, for only a small fraction of antineutrinos is expected to couple with the star. This is the *accretion* phase; we use the suffix a in the corresponding symbols.
The parameterized $\bar{\nu}_e$ flux is

$$\begin{array}{l}\Phi_a^0(t, E_\nu) = \frac{1}{4\pi D^2}\frac{8\pi c}{(hc)^3} \\ \times N_n(t)\sigma_{e^+n}(E_\nu)\; g_{e^+}(\bar{E}_{e^+}(E_\nu), T_a(t)),\end{array} \quad (13)$$

where $N_n(t)$ is the number of target neutrons assumed to be at rest and the thermal flux of positrons:

$$g_{e^+}(E_{e^+}, T_a(t)) = \frac{E_{e^+}^2}{1 + \exp\left[E_{e^+}/T_a(t)\right]} \quad (14)$$

is calculated at an average positron energy, namely $\bar{E}_{e^+}(E_\nu) = \frac{E_\nu - 1.293\text{MeV}}{1 - E_\nu/m_n}$. In the energy range of interest, $E_\nu = 5 - 40$ MeV, a simple numerical approximation of the cross section for positron interactions is

$$\sigma_{e^+n}(E_\nu) \approx \frac{4.8 \times 10^{-44} E_\nu^2}{1 + E_\nu/(260\text{ MeV})} \quad (15)$$

where the cross section is in cm^2 and E_ν is in MeV. The derivation of Eqs. 13 and 15 is given in Appendix B.

The average energy of the antineutrinos is roughly given by $5\,T_a$ and the spectrum is slightly non-thermal,[2] mostly due to the presence of the cross section σ_{e^+n}. For example, when $T_a = 1.5,\ 2.5,\ 3.5$ MeV, we get $\langle E_\nu\rangle/T_a =$

[2] The deviation from the thermal distribution can be described by a 'pinching factor'–an *effective* chemical potential introduced to distort the Fermi-Dirac thermal spectrum–in the range 4-5, that decreases when T_a increases; e.g., for $\delta E_\nu/T_a = 0.41$ the pinching factor is 4.2.

5.5, 5.2, 5.0 respectively and $\delta E_\nu/T_a = 0.39,\ 0.41,\ 0.41$ where $\delta E_\nu \equiv \sqrt{\langle E_\nu^2\rangle - \langle E_\nu\rangle^2}$. Another manifestation that the distribution is non-thermal is the scaling of the luminosity with the temperature, roughly as T_a^6–different from the thermal scaling T_a^4. In order to give some feeling of the antineutrino emission, if we suppose that at $t = 0$ we have $T_a = 2.5$ MeV and $M_a = 0.15\ M_\odot$ (see just below for a precise definition of these quantities) we get a luminosity of 1.1×10^{53} erg/s; the same luminosity and average energy would be given by a black body distribution with $T_c = 4.1$ MeV and $R_c = 82$ km.

There are two time dependent quantities in Eq. 13: the number of neutrons $N_n(t)$ and the positron temperature $T_a(t)$. It is straightforward to introduce a temperature that interpolates from an initial value to a final value:

$$T_a(t) = T_i + (T_f - T_i)\left(\frac{t}{\tau_a}\right)^m \text{ with } \begin{cases} T_i = T_a \\ T_f = 0.6\ T_c \end{cases} \quad (16)$$

where T_a denotes the *positron* temperature at the beginning of accretion (to be contrasted with T_c, the *antineutrino* temperature at the beginning of the cooling phase). With this parametrization, the positron temperature reaches $0.6\ T_c$ at $t = \tau_a$, that is what is needed to match the average antineutrino energies, namely, to ensure a continuous behavior of the average antineutrino energy (in particular at the end of the accretion phase and at the beginning of the cooling phase). The power $m = 1 - 2$ mimics the behavior found in numerical simulations; we adopt $m = 2$ as a default value.

Now we discuss the time evolution of the number of neutrons exposed to positrons $N_n(t)$, proportional to the luminosity in accretion. Our goal would be a luminosity that, at least for $t \sim 0$, decreases as $1/(1 + t/0.5\ \text{s})$. This behavior is suggested by the numerical simulations and is advocated by LL [35]. However, when we allow the temperature to vary, we vary also the luminosity, that scales as $N_n T_a^6$. Thus, we need to include an explicit factor $(T_a(t)/T_a)^6$. We arrive at our prescription for the number of neutrons exposed to thermal positrons:

$$N_n(t) = \frac{Y_n}{m_n} \times M_a \times \left(\frac{T_a}{T_a(t)}\right)^6 \times \frac{j_k(t)}{1 + t/0.5\ \text{s}}, \quad (17)$$

the fraction of neutrons being set to $Y_n = 0.6$. M_a is the initial accreting mass exposed to the positrons thermal flux. The time-dependent factor

$$j_k(t) = \exp[-(t/\tau_a)^k], \quad (18)$$

is included to terminate the accretion phase at $t \sim \tau_a$. LL use $k = 10$, which however leads to a very sharp drop of the luminosity at $t \sim \tau_a$. In our calculations, we will set instead $k = 2$, a choice that offers the advantage of leading to a smooth (reasonable, continuous) luminosity curve, closer to the type of curves found in numerical simulations. [We will show in the next section luminosity curves with $k = 10$ and with $k = 2$.]

Ultimately, the accretion phase involves 3 free parameters: M_a, T_a and τ_a, the same number of parameters of the cooling phase. Finally, we give rather generic expectations on values of these parameters: M_a is certainly lower than the whole outer core mass (about $0.6\ M_\odot$); T_a is expected to sit in the few MeV range; and, finally, the accretion should last a fraction of a second, $\tau_a \sim 0.5$ s being a typical number.

B. Avoiding composite energy spectra – time shift

In the model advocated by Lamb and Loredo and adopted for the analysis of SN1987A data, the accretion and the cooling phases are contemporaneous. This has the consequence that for times $t < \tau_a$, the antineutrino distribution is not a thermal spectrum, but a composition (=sum) of two thermal spectra, whose average energies differ by more than a factor of 2 in the best-fit point. At low energies, the spectrum is dominated by the antineutrinos from accretion; at the highest energies, by the antineutrinos from cooling.

The possibility to have a *composite spectrum* implies, among the other things, that it is easy (trivial) to reconcile the low energy events observed by Kamiokande-II and the high energy events observed by IMB in the first second: they simply belong to different and simultaneous phases of emission. We will verify this statement later by a straightforward calculation–see Table II.

We note in passing that such a composite spectrum is used in the work of Loredo and Lamb [35] but this characteristic feature is neither commented or discussed there. The compositeness of the LL spectrum (in particular, the high-energy, non-thermal tail of the antineutrinos during accretion) can be better perceived plotting it in logarithmic scale and/or by considering the time-integrated spectrum, see Fig. 2 of [63].

However, at the best of our knowledge there is no evidence from numerical simulations of a composite behavior of the spectrum; the instantaneous $\bar\nu_e$ spectrum is found to be quasi-thermal at any time and typically this property is shared also by the time-integrated spectrum; see, e.g., the discussions in [64–66]. Deviations from a thermal distribution are observed, especially during accretion [28, 67, 68]; they can be effectively described by a 'pinching' parameter of the order of a few, that means that the high-energy tail of the spectrum is depleted–not enhanced as for the composite model advocated by LL.

We believe that, in absence of an explicit indication from numerical simulations, the model that should be adopted in data analyses (and/or the null-hypothesis that should be tested) is the simplest one compatible with the numerical simulations, namely: a $\bar\nu_e$ spectrum quasi-thermal at any time–rather than, e.g., 'composite' [35], bimodal [42] or exponentially decreasing in the energy [41].

For this reason, we parameterize the total antineutrino flux by allowing for a 'time-shift' between accretion and cooling phases:

$$\Phi_{\bar\nu_e}(t) = \Phi_a(t) + (1 - j_k(t)) \times \Phi_c(t - \tau_a). \quad (19)$$

where Φ_a (resp., Φ_c) is given in Eq. 13 (resp., Eq. 10) in the case when oscillations are absent. Recalling that $j_k(t)$ appears explicitly in Eq. 17, i.e., in the accretion flux, it is clear that the effect of this function is simply to interpolate between the two phases of neutrino emission. In other words, the flux is dominated by the accretion component at $t \ll \tau_a$, the cooling phase begins around $t \sim \tau_a$ and eventually dominates the flux when $t \gg \tau_a$.

C. Limitation on τ_a

We remark the presence of a limit when the likelihood becomes unphysical. Consider the case when only the first event detected by Kamiokande-II falls in the accretion phase. If the accretion were to last a very short amount of time, $\tau_a \ll \delta t_2$, and if $t^{\rm off} \ll \delta t_2 = 0.107$ s, the antineutrino flux at the time of the first event $t = \delta t_1 = 0$ could become very large even if the number of expected number of events remains small. In this limit, the interaction rate in Eq. 3 becomes large, too. Thus, due to the factor $R(t_1, E_e, \cos\theta_1)$ in Eq. 7, the likelihood can be made arbitrarily large, because the exponential factor in the same equation (that depends on the expected number of events) will not change much.
The way to avoid this pitfall is to require a lower limit on τ_a in the numerical calculations. A limit that is adequate for the analysis of data from SN1987A is $\tau_a > 0.3$ s. We will demonstrate explicitly the presence of this unphysical behavior of the likelihood function later, when discussing its maxima.

D. Neutrino oscillations

Here we discuss the effects of (anti)neutrino oscillations on the observed $\bar\nu_e$ fluxes. The survival probability P for $\bar\nu_e$ emitted by supernova is dictated by two different interactions with the star medium. The first is the usual matter effect [64, 69] of charged current interactions between $\bar\nu_e$ and the electrons of the matter. The second is the effect of $\nu - \nu$ interactions [70–74], that is known to be important in specific cases [75, 76] and whose behavior has been quantified in certain approximations [77–80].

In order to describe oscillations we have to distinguish the two arrangements of the neutrino mass spectrum that are compatible with the present knowledge of neutrino properties (see, e.g., [82]):
For **normal** mass hierarchy the survival probability and the observed $\bar\nu_e$ flux are:

$$\begin{aligned} P &= U_{e1}^2, \\ \Phi_{\bar\nu_e} &= P\ \Phi^0_{\bar\nu_e} + (1-P)\ \Phi^0_{\bar\nu_\mu}, \end{aligned} \tag{20}$$

where we recall that Φ^0 is the flux in absence of oscillations. We have assumed that $\Phi^0_{\bar\nu_\mu} = \Phi^0_{\bar\nu_\tau}$ and each term is the sum of the cooling flux and accretion flux.
The $\nu - \nu$ interaction is most relevant for **inverted** mass hierarchy [77–80, 83, 84]. As an example the electron antineutrino survival probability given in [80] is:

$$\begin{aligned} P &= U_{e1}^2(1-P_f) + U_{e3}^2 P_f, \\ \Phi_{\bar\nu_e} &= P\ \Phi^0_{\bar\nu_e} + (1-P)\ \Phi^0_{\bar\nu_\mu}. \end{aligned} \tag{21}$$

note that $P_f \to 1 - P_f$ if $\nu - \nu$ interactions were not included ('spectral swap') [81]. We adopt the usual decomposition of the mixing elements in terms of the mixing angles: $U_{e3} = \sin\theta_{13}$ and $U_{e1} = \cos\theta_{12}\cos\theta_{13}$ with $\theta_{12} = 35^\circ \pm 4^\circ$ and $\theta_{13} < 10^\circ$ at 99 % C.L. For the measured solar oscillation parameters, the Earth matter effect is known to be small (see, e.g., [85]). We include it in the analysis anyway evaluating the survival probabilities with the PREM model [86].

In the case of normal mass hierarchy the probability $P \sim 0.7$ is reliably predicted and rather precisely known. Instead, for inverted mass hierarchy, P depends strongly on the unknown mixing angle θ_{13}. In fact, the flip probability P_f (that quantifies the loss of adiabaticity at the 'resonance' related to the atmospheric Δm^2) is:

$$P_f(E_\nu, \theta_{13}) = \exp\left[-\frac{U_{e3}^2}{3.5\times10^{-5}}\left(\frac{20\ \text{MeV}}{E_\nu}\right)^{2/3}\right], \tag{22}$$

where the numerical value corresponds to the supernova profile $N_e \sim 1/r^3$ given in [69]. The predictions for the $\bar\nu_e$ flux in the detector could be tested with a relatively large amount of data: a galactic supernova could turn out to be useful to discriminate the right mass hierarchy.

As a default, we assume that an equal amount of energy goes in each species (equipartition hypothesis) during cooling. Furthermore, we suppose that the temperature of $\bar\nu_\mu$ and $\bar\nu_\tau$ is in a fixed ratio with the $\bar\nu_e$ temperature. Following [68] we assume:

$$T(\bar\nu_\tau)/T(\bar\nu_e) = T(\bar\nu_\mu)/T(\bar\nu_e) = 1.2, \tag{23}$$

We tested that a value in the 1.0-1.5 or a deviation of the amount of energy stored in non-electronic neutrino species by a factor of 2 does not affect crucially the fitted antineutrino flux. In the accretion phase, we will suppose that only ν_e and $\bar\nu_e$ are emitted in equal amount, whereas $\Phi^0_a(\bar\nu_x) = 0$. The fit provides a reasonably fair description of the antineutrino flux anyway, but the estimation of the amount of energy emitted during accretion should be considered as a lower bound.

E. Summary of the parameterization of the flux

In this section, we proposed a new parameterization of the antineutrino flux. Our aim is fourfold: 1) to improve on the parameterizations used in the previous analyses, getting closer to the energy spectra observed in numerical simulations; 2) to include flavor oscillations in a complete analysis of SN1987A data; 3) to test whether the

choice of the parameterization is important (the straightforward analysis of SN1987A data discussed below suggest that this is so); 4) and finally, to stimulate further work in the direction of finding a parameterized form of the neutrino emission.[3] We will check with explicit calculations that our conclusions are stable even when we change in wide reasonable ranges the model parameters for which we adopt default values (such as $T(\bar{\nu}_\tau)/T(\bar{\nu}_e)$ in Eq. 23, deviations from the equipartition hypothesis, the parameter m in Eq. 16 and the parameter k in Eq. 18–see Sect. IV B 6 c).

IV. RESULTS

In the previous two sections we constructed, step by step, a likelihood function that represents the probability function of the overall data set. This probability varies in the parameters space and depends on the model for the antineutrino emission. As anticipated, one of the main goal of this paper is to verify whether the best-fit values of the parameters, that maximize the likelihood function, are physically acceptable. Quite evidently, the answer does depend on the model selected for data analysis.

Before proceeding, a brief note on the adopted statistical tools is in order. We remark that LL adopted a Bayesian analysis while we use a frequentist approach, which occasionally leads to some difference in the confidence levels, but not in the best fit points. More specifically to calculate the error on one parameter we use as a rule the profile likelihood, namely the likelihood evaluated fixing the parameter of interest and maximizing the other (nuisance) parameters. A similar procedure allows us to calculate the confidence regions.

The structure of this section is the following: in Sect. IV A we describe the simpler (one component) model, in Sect. IV B we describe the more complete (two components) model. This second part illustrates the impact of each improvement in the description of the flux; the final result is discussed in detail in Sect. IV B 6.

A. One component model

Here we list the results of the likelihood maximization procedure when we include only the cooling phase. This model has 6 parameters: the $\bar{\nu}_e$ temperature T_c, the duration τ_c, the neutrinosphere radius R_c and the three detector offset times $t^{\rm off}$. It is identical to the "Exponential cooling model" reported in [35], also termed "minimum" or "standard" model in [26]. The comparison of the best-fit values of LL ($R_c = 40$ km, $T_c = 3.81$ MeV, $\tau_c = 4.37$ s and $t^{\rm off} = 0$ s [35]) with our results

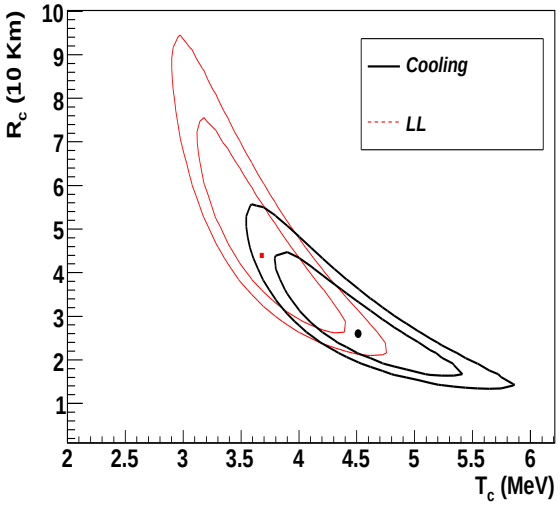

FIG. 1: *Two dimensional confidence regions for the cooling parameters R_c and T_c. The gray (red) contours are the exponential cooling result (68% and 90% C.L.) following Loredo and Lamb analysis. The dark contours are our result for one component cooling model. The best fit points are also displayed.*

($R_c = 44$ km, $T_c = 3.68$ MeV, $\tau_c = 4.43$ s and $t^{\rm off} = 0$ s) is satisfactory, the agreement being at the level of 10%.

Even the two dimensional confidence regions and the 95% C.L. errors on the parameters agree to within 20%, which is remarkable since they have been obtained with completely different statistical procedures: frequentist in our case, Bayesian in the case of LL. This suggests that the statistical procedure has a minor impact on the inferences. We will see that more relevant changes are induced by certain technical improvements; even more important are the changes induced by the new emission models, discussed later.

We proceed and quantify the impact of the technical improvements in the likelihood, described in Sect. II.
The inclusion of the detection efficiency $\eta(E_{e^+})$ as done in Eq. 7 gives the single most important change in the results. In fact we obtain:

$$R_c = 30 \text{ km}, T_c = 4.21 \text{ MeV}, \tau_c = 3.88 \text{ s}. \quad (24)$$

Using the new cross section $\sigma_{\bar{\nu}_e p}(E_{\nu_e})$ for the inverse beta decay we get the new best-fit point values:

$$R_c = 26 \text{ km}, T_c = 4.58 \text{ MeV}, \tau_c = 3.72 \text{ s}. \quad (25)$$

Our assumption on the background B_i has a little effect on these values that become $R_c = 26$ km, $T_c = 4.59$ MeV and $\tau_c = 3.81$ s.
Similarly the inclusion of the event directions, $\cos\theta_i$ (Eq. (20) in [57]), that produces:

$$R_c = 26 \text{ km}, T_c = 4.47 \text{ MeV}, \tau_c = 3.88 \text{ s}. \quad (26)$$

[3] This will be of great importance to interpret the experimental signal from a future supernova.

The values of $t^{\rm off}$ parameters are always zero in these models, and it is easy to convince oneself that this is due to the fact that, in this one component model, the signal is forced to decrease with the time.

The larger change concerns the radius R_c that diminishes by 35% in comparison to the value given by Lamb and Loredo, approaching the expected neutron star radius, but still twice larger than a typical value. In Fig. 1 we show the contour plots in the $R_c - T_c$ plane, the two parameters that show the largest correlation among them. In gray (red) we draw the 68% and 90% contours level that we obtain adopting the same likelihood function of LL, in black the contours level when we construct the likelihood function following Sec. II, i.e., including all the structural improvements discussed above.

With the best-fit points it is possible to estimate the total energy emitted by neutrinos in this model. Hypothesizing that in the cooling phase all types of neutrinos are emitted, each one carrying away an equal amount of energy, the total energy is:

$$\frac{E_c}{10^{53}\text{erg}} = 3.39 \times 10^{-6} \int_0^\infty dt \left(\frac{R_c}{\text{km}}\right)^2 \left(\frac{T_c(t)}{\text{MeV}}\right)^4 , \quad (27)$$

This value should be comparable with the gravitational binding energy of the new born neutron star, $E_b = (1-5)\cdot 10^{53}$ erg. The LL result for exponential cooling model is $E_b = 5.02\cdot 10^{53}$ erg, namely a binding energy at the upper limit of this range, whereas our results $E_b = 3.55\cdot 10^{53}$ erg is included in the expected range.

Incidentally, the results in eqs. 24, 25 and eqs. 26 are also in pretty good agreement with those described in the Bahcall book [26]; more discussion on this comparison is given in [62].

B. Two components model

Now we include both emission phases. Following the order of Sect. III, we improve, step by step, the emission model of the accretion phase. To describe accretion we add 3 new physical parameters, namely: the positrons temperature T_a, the duration of the accretion phase τ_a and the initial accreting mass M_a. So the likelihood becomes a function of 9 parameters, rather than 6 as for the one component model. The best fit results are given in Table I and will be commented in details below.

The last column of Table I shows the values

$$\Delta\chi^2 = \chi^2_c - \chi^2_m, \quad (28)$$

where χ^2_c is calculated with the best one-component model of the previous section, i.e., the last case of previous subsection (Eq. 26), and χ^2_m is calculated with the best-fit model described in the section indicated in each line of Table I. The larger the difference, the larger the evidence for accretion. A quantitative evaluation of the evidence, taking into account the increased number of parameters, will be provided in Sect. IV B 6 a. We anticipate that for all model, the evidence is stronger than the conventional 5%.

Sect.	R_c [km]	T_c [MeV]	τ_c [s]	M_a [$M_\odot$]	T_a [MeV]	τ_a [s]	$t^{\rm off}$ [s]	$\Delta\chi^2$
II	12	5.46	4.25	5.59	1.52	0.72	0.	14.7
III A	14	4.99	4.76	0.82	1.75	0.67	0.	11.2
III B	14	4.88	4.72	0.14	2.37	0.58	0.	9.8
III D	16	4.62	4.65	0.22	2.35	0.55	0.	9.8

TABLE I: *The best-fit values of the astrophysical parameters for two components model neutrino emission. Each line of this table is an incremental step toward the final improved parameterization. The last column shows the difference between the χ^2 of our one-component (cooling) model and the χ^2 of each two-component model.*

1. *Effect of the new likelihood–improvements of Sect. II*

The first line of Table I shows the best-fit results obtained using the likelihood function constructed in our Sect. II and one of the emission model used by LL, namely the model called "Exponential cooling and truncated accretion" (later called ECTA) [35]. We see that the best-fit value for the initial accreting mass M_a is very large and hardly acceptable on physical basis: this parameter is restricted by $M_a < 0.6 M_\odot$ for the reasons mentioned in Sect. III A 2. This result, however, is in agreement with what found by Lamb and Loredo, who fixed $M_a \equiv 0.5\ M_\odot$ in all models of their Table V, namely they inserted a "prior" in their analysis. This assumption reduces to 8 the number of free parameters and produces these best-fit values:

$$\begin{array}{c} R_c = 12 \text{ km}, \quad T_c = 5.40 \text{ MeV}, \quad \tau_c = 4.40 \text{ s}, \\ M_a \equiv 0.5\ M_\odot, \quad T_a = 2.02 \text{ MeV}, \quad \tau_a = 0.70 \text{ s} \end{array} \quad (29)$$

with $\Delta\chi^2 = 13.4$. We call this best-fit point LL^* to distinguish it by the true global maximum of likelihood function, shown in Table I. In passing, we note that our structural improvements of the likelihood do not radically change the conclusions of Lamb and Loredo [81].

2. *New spectrum and $T_a(t)$–improvements of Sect. III A*

The second line of Table I shows that there is less need of the *a priori* on M_a when we exploit the correct parametrization of the accretion flux (accounting for the right kinematics of e^+n process, using the new cross section and allowing the positron temperature to increase with the time). In fact the best fit value for the initial accreting mass decreases to $M_a = 0.82\ M_\odot$ in this model, a value that is a bit larger than the reference outer core mass, $0.6\ M_\odot$, but now closer to the expected

range. The accretion phase is characterized by a low mean energy and by a duration shorter than a second, as expected. The total energy carried in each phase is: $E_c = 2.0 \cdot 10^{53}$ erg and $E_a = 5.7 \cdot 10^{52}$ erg, and the total binding energy is $E_b = E_a + E_c = 2.5 \cdot 10^{53}$ erg. It is important to note that, in this model and as in the LL model (see Sect. III B) the two emission phases are contemporaneous. This implies that the emission spectrum is 'composite', a features that makes it easier to account for the difference between the average energies of IMB and of Kamiokande-II, as can be seen from the relatively high value of $\Delta\chi^2$ in Table I.

3. *Separating accretion and cooling–improvements of Sect. III B*

In Sect. III B we discussed a procedure ('time shift') to separate temporally the accretion and cooling phases. The time shift produces two families of best fit values: when the IMB data fall in the accretion phase ($t^{\rm off}_{\rm IMB} \sim 0$) the positron temperature T_a has to increase; when the IMB data fall in the cooling phase ($t^{\rm off}_{\rm IMB} \sim \tau_a$) the temperature T_a can remain relatively low. We show in Fig. 2 the likelihood profile of T_a parameter, where the above situation becomes evident.[4] The figure refers to final model that includes also neutrino oscillations, but the same structure arises already as soon as the time-shift is included. The other local maximum of the likelihood besides the one shown in Table I is at:

$$\begin{array}{lll} R_c = 10 \text{ km}, & T_c = 5.28 \text{ MeV}, & \tau_c = 4.74 \text{ s}, \\ M_a = 1.27\ M_\odot, & T_a = 1.65 \text{ MeV}, & \tau_a = 1.4 \text{ s} \end{array} \quad (30)$$

with $t^{\rm off}_{\rm IMB} = 0.93$ s and $\Delta\chi^2 = 10.2$. The χ^2 values obtained with this best-fit solution is very near to best-fit value shown in Table I, the difference being only ~ -0.5. Therefore this solution cannot be discarded on statistical basis. Thus, let us examine the physical content of this solution. When the data of IMB belong to cooling phase, as in this solution, the value of T_a diminishes to account for the mean energy of the first KII events, and the initial accreting mass M_a increases to achieve the right number of detected events. This implies that the family of solution with a time-shift different from zero has larger values of M_a. The solution of Eq. 30 has a time constant τ_a two-three times larger that the expectations and, more importantly, it has a value M_a twice the outer core mass; instead, the solution of Table I has a completely acceptable value of M_a. Since we expect that only a fraction of the outer core mass is exposed to the thermal positron flux, we are led to believe that the latter solution is more plausible than the former.

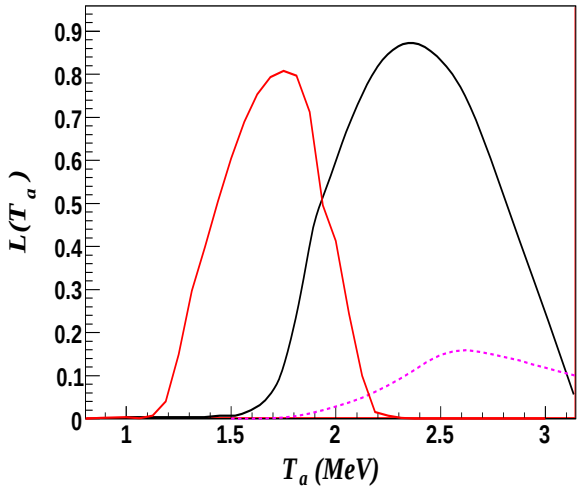

FIG. 2: *Profiles likelihood for T_a parameter of accretion with the complete emission model (III D). The red line is the family of solutions with $t^{off}_{IMB} \simeq 0.5$ s. The dark line is the other family of solutions with $t^{off} = 0$ and $M_a < 1 M_\odot$. The dotted line is the unphysical family of solutions discussed in Sect. III B with $\tau_a = 0.2$ s.*

4. *Effects of oscillations–improvements of Sect. III D*

In the last line of Table I, we complete the parameterization of the flux by including (anti)neutrino oscillations. The solution is very similar to the one described in the previous section and the astrophysical parameters are rather similar to the expectations. The total energy emitted by neutrinos in each emission phase is: $E_c = 1.8 \cdot 10^{53}$ erg and $E_a = 4.8 \cdot 10^{52}$ erg and the total binding energy is $E_b = 2.2 \cdot 10^{53}$ erg. The best-fit values have been obtained for normal hierarchy and with the assumptions discussed in Sect. III D. The flux of $\bar\nu_e$ that reaches the detectors is a combination of the $\bar\nu_e$ and $\bar\nu_\mu$ emitted within the star. The best-fit values showed in the table refers to the radius and temperature of $\bar\nu_e$, that however are closely related to the $\bar\nu_\mu$ values. In fact the temperature of emission is $T_c(\bar\nu_\mu) = 5.5$ MeV (due to Eq. 23) and the radius of $\bar\nu_\mu$ neutrinosphere is $R_c(\bar\nu_\mu) = 10$ km (due to equipartition).

The assumption that we can neglect the ν_μ during accretion implies that the accretion flux is suppressed by the factor $P = \cos^2\theta_{12} \sim 0.7$, so the best-fit of initial accreting mass has to increase by $1/P$ to maintain the same fit. This quantitative change has some impact on the interpretation of the multiple solutions: In fact, the family of solutions with $t^{\rm off}_{\rm IMB} \neq 0$ s and with lower values T_a (red line of Fig. 2) turns out to be characterized by values of M_a greater than 1 $M_\odot$. Thus, physical consid-

[4] In technical terms, the case when there are multiple maxima of similar quality is termed as pathological likelihood. The statistical concept of 'pathological' solution should be distinguished from the concept of 'unphysical' solution; e.g., the one corresponding to dotted line of Fig. 2 and explained in Sect. III B.

erations on the meaning of the accreting mass suggest, as more plausible, the family of solutions shown with a dark line in Fig. 2 and in the last line of Table I.

5. What happens with inverted mass hierarchy?

For inverted mass hierarchy, the effects of $\nu - \nu$ interactions are known to be relevant but their quantitative treatment is still under discussion, see e.g., [83, 84]. This consideration, already, prevents us to draw firm conclusions. However, adopting the formulae given in Sect. III D to illustrate which are the possible effects, we can distinguish 2 main cases: large values of θ_{13}, namely $\theta_{13} > 0.5^\circ$ and small values of θ_{13}, namely $\theta_{13} < 0.1^\circ$. In the first case, $P_f \sim 0$ and the survival probability $P = U_{e1}^2$; thus, we find the same results as for normal hierarchy.

In the second case, the flip probability is $P_f \sim 1$ and $P = U_{e3}^2$ in Eq. 21. The suppression of the $\bar{\nu}_e$ survival probability $P \sim 0$, along with the assumption that the flux of $\bar{\nu}_\mu$ and $\bar{\nu}_\tau$ are very small during accretion, implies the *absence* of electron antineutrino events during accretion. Such a hypothesis can be tested with–and, to some extent, excluded by–SN1987A observations [81]. (Note that neglecting $\nu - \nu$ interaction, the condition $P \sim 0$ turns out to be realized in the other case, namely for *large* values of θ_{13} [81].) Certainly, this result for inverted hierarchy should be taken with great caution for it depends crucially not only on the present understanding of the effects of $\nu - \nu$ interactions but also on the incomplete description of the flux of $\bar{\nu}_\mu$ and $\bar{\nu}_\tau$ during accretion.

It is interesting to note that certain hints from the analyses of oscillation suggest that θ_{13} is relatively large [87]. In view of the discussion just above, this would mean that there is no need to distinguish between the two mass hierarchies, and the treatment of oscillation would be thus simplified.

6. Remarks on the two component models

Having calculated the best fit values of the two component model, and having understood their meaning, we pass to discuss: (a) the evidence for the accretion phase (namely, we compare the two component and the one component model); (b) the errors on the best fit parameters for the improved model; (c) the stability of the results; (d) the difference between the best-fit ECTA model and our improved model; (e) the *a posteriori* information on the background.

a. Evidence for the phase of accretion In order to test whether the $\Delta\chi^2$ of the models with accretion (Table I) are just an effect of fluctuations, we perform a standard likelihood ratio significance test[5] [89]. For the four models of Table I, we find that we can reject the null hypothesis (=no accretion) with a significance level of $\alpha = 0.2\%$, $\alpha = 1.1\%$, and $\alpha = 2.0\%$ (for the last two models) respectively. Three remarks are in order:
(1) The result $\alpha = 0.2\%$ basically agrees with the claim of Lamb and Loredo: the ECTA model for emission, if correct, would lead to an important evidence for accretion. Our improvements in the likelihood (described in Sect. II) do not change this inference significantly.
(2) Also the other models permit to exclude the 'null hypothesis' that we test (namely, the absence of an accretion phase) with the conventional 5% criterion. But the evidence becomes a bit weaker and if one prefers to be very conservative, this could suggest caution. This outcome can be easily understood by the fact that our model for accretion is more constrained and can account for certain features of the data (such as the difference of IMB and KII energies) only at the price of some tension, that is reflected by the increased value of α.
(3) Obviously, even the conservative attitude does not forbid us to use the SN1987A data to learn something on accretion. It is the question that we formulate that changes: if we *assume* that the accretion phase exists, we can ask the data to determine the model parameters.

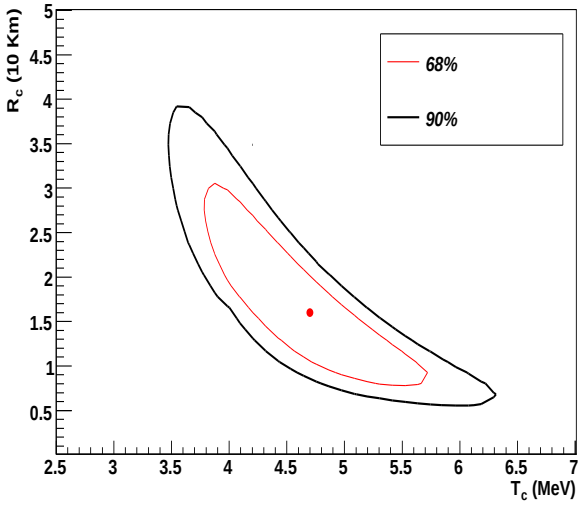

FIG. 3: *Two dimensional confidence regions for cooling parameters R_c and T_c of $\bar{\nu}_e$ with the complete emission model (III D).*

[5] We calculate $\alpha = \prod_{i=1}^{\nu} \int \exp(-x^2/2)/\sqrt{2\pi} dx_i$ for $\sum_{i=1}^{\nu} x_i^2 > \Delta\chi^2$ and taking $\Delta\chi^2$ from Table I, where the number of random variables x_i equals the new degrees of freedom $\nu = 3$.

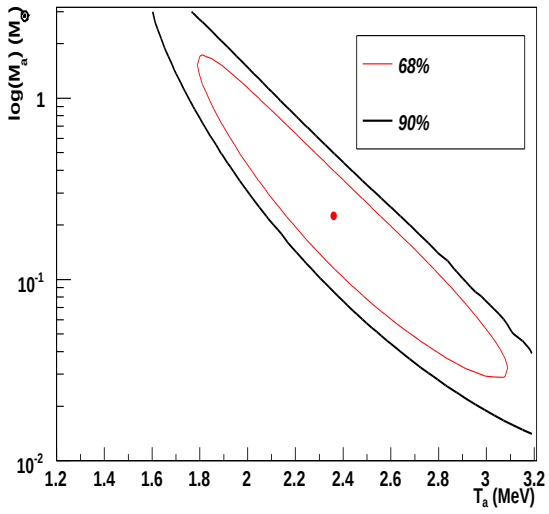

FIG. 4: *Two dimensional confidence regions for accretion parameters M_a and T_a of $\bar{\nu}_e$ with the complete emission model (III D).*

b. Errors on the parameters The 1σ errors obtained by a conventional, $\Delta\chi^2 = 1$, Gaussian procedure [89] are:

$$\begin{aligned} R_c &= 16^{+9}_{-5} \text{ km}, & M_a &= 0.22^{+0.68}_{-0.15}\ M_\odot, \\ T_c &= 4.6^{+0.7}_{-0.6} \text{ MeV}, & T_a &= 2.4^{+0.6}_{-0.4} \text{ MeV}, \\ \tau_c &= 4.7^{+1.7}_{-1.2} \text{ s}, & \tau_a &= 0.55^{+0.58}_{-0.17} \text{ s}. \end{aligned} \quad (31)$$

The 1 sided, 1σ errors for the offset times (obtained by integrating the normalized likelihood profile [89]) are:[6]

$$t^{\rm off}_{\rm KII} = 0.^{+0.07} \text{ s}, t^{\rm off}_{\rm IMB} = 0.^{+0.76} \text{ s}, t^{\rm off}_{\rm BAK} = 0.^{+0.23} \text{ s}. \quad (32)$$

The couples of parameters that are more tightly correlated between them are T_c with R_c, and M_a with T_a. In Fig. 3 and Fig. 4 we report the two dimensional confidence regions for these couples of parameters showing the 90% and 68% contour levels; the correlations are quite evident from the figures. In these figures we focused on the family of solutions with $t^{\rm off} = 0$ after testing that the other maxima have a very large value of accreting mass, as discussed in Sect. IV B 4.

c. Stability of the best-fit values In order to show the stability of our result we investigated:
1) different values for the exponent $m = 1$, 3, 4 (rather than $m = 2$) in Eq. 16, that describes the temporal behavior of positron temperature during accretion;
2) the value $k = 10$ (rather than $k = 2$) in Eq. 18 that describes the sharpness of the transition between accretion and cooling phases;
3) deviations from the hypothesis of equipartition, by increasing or decreasing the ratio between the $\bar{\nu}_e$ and $\bar{\nu}_x$ luminosities by a factor of 2 [68].
In all cases, the χ^2 changes less than 1 with respect to the best fit result; furthermore, the best fit values of the astrophysical parameters change only within their 1 σ errors given in Eq. 31.

[6] Only IMB had a reliable measurement of the absolute times; thus, we can use the time of its first event along with $t^{\rm off}_{\rm IMB}$ to infer the moment of the beginning of the collapse, presumably coincident with the emission of an intense gravitational wave.

event	δt_i [s]	E_i [MeV]	LL^*	III D
K1	$\equiv 0.0$	20.0	0.69	1.00
K2	0.107	13.5	0.92	1.00
K3	0.303	7.5	0.93	0.81
K4	0.324	9.2	0.95	0.93
K5	0.507	12.8	0.89	0.84
K6	0.686	6.3	0.66	0.10
I1	$\equiv 0.0$	38	0.02	1.00
I2	0.412	37	0.02	0.55
I3	0.650	28	0.05	0.48
B1	$\equiv 0.0$	12.0	0.94	0.99
B2	0.435	17.9	0.70	0.85

TABLE II: *Accretion probabilities for the events occurred in the first second; all the other events have a probability to be due to accretion lower than 5%. The first three columns identify the individual events. The last two columns are the probabilities that an event is due to accretion. The model used in the fourth column includes the improvements of Sect. II and following LL sets $M_a = 0.5\ M_\odot$; the one used in the fifth column includes also the improvements of Sect. III D.*

d. On the differences with the parameterization by Lamb and Loredo To illustrate better the difference between the ECTA model and our final emission model, we show in Table II the probabilities of the individual events to be due to accretion. (Fig. 7 of Ref. [62] is a viewgraph corresponding to the results of this Table.) A direct comparison with LL results [35] is not possible, since a similar table is not given there; thus, we repeat their calculation following their prescriptions and make reference to the model LL^* described in Sect. IV B 1.
The column denoted by LL^* (fourth column)–the model defined in Eq. 29–shows that the early KII and Baksan events are due to accretion and those by IMB to cooling. This proves that, assuming the Lamb and Loredo ECTA model, the fit takes advantage of the fact that the assumed energy distribution is 'composite': the low energy events of KII are explained by the accretion component, the high energy events of IMB instead by the high energy tail due to the cooling component.
The results of our model are shown in the column of Table II (fifth column) denoted by III D. Since our model has (by construction) a quasi-thermal spectrum at any time, both KII and IMB early events have a large probability to be due to accretion. The tension between the different energies of KII and IMB events leads to a slightly worse

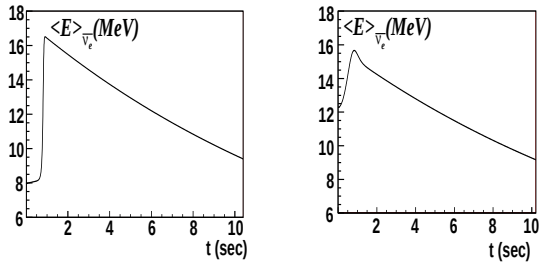

FIG. 5: *$\bar{\nu}_e$ mean energy as a function of the time in the LL ECTA model (left panel) and in the III D model (right panel).*

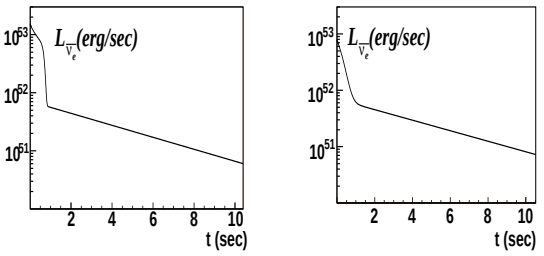

FIG. 6: *$\bar{\nu}_e$ luminosity in the LL ECTA model (left panel) and in the III D model (right panel).*

χ^2, see Table I.

Finally, we compare in Fig. 5 the mean energy of $\bar{\nu}_e$ in the LL^* accretion model, left panel, with the trend of the mean energy in our model III D, right panel, whereas in Fig. 6 we plot the $\bar{\nu}_e$ luminosity obtained with the LL^* model (left panel) and the model of Sect. III D (right panel). The features of these curves are similar to those found in typical numerical simulations, see e.g. [13], with the exception of the average energy curve of the LL model that has a very pronounced jump.

e. Information on background events We are now in the position to obtain interesting information on the background. First of all, we can evaluate the *a posteriori* probabilities that an individual event is due to background. Since the discussion of the background of Baksan detector is already included in [88], we will focus on the discussion of the background in the KII detector, extending and complementing our previous calculations [43].

The sixth event of Kamiokande-II (K6) is particularly interesting; from Table VI of LL, we see that it has only 15% probability to be due to background. This probability doubles when we include the structural improvements of the likelihood (Sect. II) mostly due to the new background discussed in [43], and increases again to 85% after the emission models improvements of Sect. III D. Thus, the improved model suggests that the event K6 should not be attributed to accretion, as in the first and most popular interpretation [17] that considers the fact that the event K6 is below the threshold of 7.5 MeV. The reason is that, in the improved model, the energy of the antineutrinos is expected to be maximal at $t \sim 0.5$ s.

Similarly, we find that the events K13-K16 (usually not included in data analysis) are almost certainly due to background.

Next, using the techniques introduced in [43] we can evaluate the *a posteriori* probability to have n background events. For the Kamiokande-II dataset we get 10% for $n = 5$, 35% for $n = 6$, 44% for $n = 7$, 10% for $n = 8$, that is not in disagreement with the expectation $\bar{n} = 5.6$ in the whole energy range. Thus, it is not impossible that there was another background event besides the events K6 and K13-K16, that can be compared with the expectation of 0.66 background events Kamiokande-II, in a time window of 30 seconds and above the 7.5 MeV energy threshold. Finally, we note that the probability to have $n = 16$ (that is, the hypothesis that no signal from SN1987A was detected) is as low as 11σ. This is a reassuring result and it is again in agreement with the quantitative evaluation of 10σ in [43].

V. SUMMARY

We presented an improved analysis of observations of SN1987A by Kamiokande-II, IMB and Baksan. We recall the main points:

1. We collected in Sect. II a large number of technical improvements: new detection cross section, procedure to include the information on the direction of the events, treatments of the background and of the efficiency. The most relevant improvement is the last one, but none of these changes affect SN1987A data analysis in a crucial manner.

2. We described in Sect. III D the various effects of (anti)neutrino oscillations: the oscillations in the star (including the self interaction of neutrinos) and the Earth matter effect. We verified that oscillations with normal hierarchy do not affect the results in an essential manner and discussed the inverted hierarchy case.

3. We proposed in Sect. III a new parameterization of the flux of electron antineutrinos emitted in the accretion phase. We improved on the energy spectrum, and most importantly, on the time-distribution: (a) We prescribed the temperature of the positrons to increase in such a manner that at $t \sim \tau_a$ the average energy antineutrinos is approximatively continuous, that overcomes a shortcoming of the parameterization of [35] noted in [41] and recalled in the Introduction. (b) We also prescribed that the number of neutrons exposed to the positron flux decreases in time more smoothly than as in [35]; in this way the luminosity is also continuous, as expected on general basis. (c) Finally, we avoided the simultaneous presence of cooling and accretion antineutrinos by time-shifting (delaying) the cooling phase of an amount $t \sim \tau_a$, again improving on the previous parameterizations adopted for the analyses of SN1987A events.

4. We demonstrated that the improvements on the parameterization are the most important. The most striking feature is that the best fit parameters are rather similar to the expectations of the Bethe and Wilson scenario. This is in contrast with what happens using the

Lamb and Loredo parameterizations of the flux, where it is needed to impose a prior in the analysis to avoid best-fit values outside the physical ranges. Furthermore, our flux leads to smooth luminosity curves and average energies. [The most appealing outcomes of their analysis, such as the neutrino sphere radius resembling the neutron star mass, the duration of the accretion phase ~ 0.5 s, the total amount of emitted energy, remain practically unchanged.]

5. We evaluated the errors and the correlations on the parameters and we can rule out the hypothesis of a one-phase model with a significance of 2%.

From these calculations one draws two main messages: an accurate choice of the model to be adopted for the analysis of SN1987A observations is quite important; the agreement between the observations and the conventional expectations is more than encouraging in the proposed model. We hope that these results will help to progress further in the understanding of this epochal observation.

Acknowledgments

We thank A. Drago and D.K. Nadyozhin for discussions on astrophysics, E. Lisi, A. Strumia, F. Terranova and F.L. Villante for discussions on the treatment of efficiency, and S. Pastor and A.Yu. Smirnov for discussions on oscillations. We are grateful to the anonymous Referees for useful remarks. The work is partly supported by the High Energy Astrophysics Studies contract number ASI-INAF I/088/06/0, the MIUR grant for the Projects of National Interest PRIN 2006 "Astroparticle Physics" and by the European FP6 Network "UniverseNet" MRTN-CT-2006-035863. Preliminary results have been presented in [81] and discussed in conferences, e.g., [63], [88] and [62].

Appendix A: Form of the Likelihood

In this section we construct the likelihood of a data set of supernova positrons collected by a certain detector, for example, a water Cherenkov detector. We will consider the possibility that an event can be missed and describe the fact that the reconstructed energy is in general different from the true one. We focus the discussion on the energy of the events, for the relative time is precisely measured and the error on the direction is negligible in comparison to the wide angular distribution, characteristic of the inverse beta decay reaction.

The N_d data are characterized by their detection times t_i, that we suppose known without error, and other measured features. As mentioned above, we focus the discussion on the energy of the positron, E. The overall data set extends over a time interval T and we can split up this interval in many small time bins, each one of size $\delta t \ll T$. Also the energy interval is binned, and the size of each bin is denoted with δE.

The probability for the data collected, i.e., the likelihood function of data set, is $\mathcal{L} = \prod_{i=1}^{N} P_i$ where

$$P_i = \begin{cases} P(d^0) \text{ if the } i\text{-th bin has 0 events} \\ P(d(E_i))\ \delta E \text{ if the } i\text{-th bin has 1 event,} \end{cases} \tag{A1}$$

and where the number of bins is much larger than the number of detected events, $N \gg N_d$.

1. Probability to detect no event. Efficiency

The probability of non detection can be calculated taking into account the several situations that can result in a non-detection. Furthermore we can distinguish between the signals associated to SN neutrinos, called s, and the background signals, called b. Using the trick of "extending the conversation", we get, $P(d^0) = \sum_{m=0}^{\infty} \sum_{n=0}^{\infty} P(d^0, s^m, b^n)$, that is the probability that m positrons are produced by SN neutrinos, n events of background occurred and no event is detected. Since the intervals δt are small we neglect the terms involving more than one event occurring in δt

$$P(d^0) \simeq\ P(d^0, s^0, b^0) + P(d^0, s^0, b^1) + P(d^0, s^1, b^0). \tag{A2}$$

Using the well known product rule of probability (namely, $P(A, B \mid C) = P(A \mid B, C)P(B \mid C)$) we begin calculating the simplest case when no events are present

$$P\left(d^0, s^0, b^0\right) = P(d^0, s^0 \mid b^0)P(b^0) = P(d^0 \mid s^0, b^0)\cdot \\ P(b^0)\cdot P(s^0) = e^{-B\delta t}\cdot e^{-S(t)\delta t} \simeq 1 - \delta t[S(t) + B], \tag{A3}$$

where we neglect the $O(\delta t^2)$ terms. We introduce here the positron production rate $S(t)$, the time independent *measured* background rate B and we assumed Poisson statistics for both processes. The next term is the probability that no events are detected and 1 background event occurs. This is by definition set to zero $P(d^0, s^0, b^1) \equiv 0$. This definition means that the background is a detected event that is not due to the SN neutrino signal. The background rate, assumed to be time independent, can be measured by the experimental collaborations in the instants of time when the signal is known to be absent. The last term is more complicate. The probability that one positron due to SN neutrino was produced but no events were detected is

$$P(d^0, s^1, b^0) = \int dE\ P(d^0, s(E), b^0) = \\ \int dE\ P(d^0, s(E) \mid b^0)\cdot P(b^0) = \\ \int dE\ P(d^0 \mid s(E), b^0)\cdot P(b^0)\cdot P(s(E)) = \\ \int dE\ (1 - \eta(E))\cdot e^{-B\delta t}\cdot S(t, E)\delta t e^{-S(t,E)\delta t} \simeq \\ (1 - B\delta t)\int dE(1 - \eta(E))S(t, E)\delta t(1 - S(t, E)\delta t) = \\ \int dE\ S(t, E)\delta t - \int dE\ \eta(E)S(t, E)\delta t + O(\delta t^2) = \\ (S(t) - R(t))\delta t, \tag{A4}$$

where we used the symbol

$$S(t) \equiv \int dE\ S(t,E) \tag{A5}$$

to denote the positron *production* rate and

$$R(t) \equiv \int dE\ R(t,E) \equiv \int dE\ \eta(E) S(t,E) \tag{A6}$$

to denote the positron *detection* rate. In equation A4, we introduce the function

$$P(d^0 \mid s(E), b^0) = 1 - \eta(E), \tag{A7}$$

that defines the detection efficiency function, assumed to be time independent. Collecting the various terms, we conclude that the total probability of non-detection is

$$\begin{array}{l} P(d^0) = P(d^0, s^0, b^0) + P(d^0, s^0, b^1) + P(d^0, s^1, b^0) \simeq \\ 1 - \delta t(S(t) + B) + \delta t(S(t) - R(t)) \simeq e^{-(B+R(t))\delta t} \end{array} \tag{A8}$$

2. Probability to detect one event. Smearing

Now we must calculate the probability of the intervals where detection occurred:

$$P(d(E_i)) \simeq P(d(E_i), s^1, b^0) + P(d(E_i), s^0, b^1) \tag{A9}$$

We begin from the first term:

$$\begin{array}{l} P(d(E_i), s^1, b^0) = \int dE\ P(d(E_i), s(E), b^0) = \\ \int dE\ P(d(E_i), s(E) \mid b^0) \cdot P(b^0) = \\ \int dE\ P(d(E_i) \mid s(E), b^0) \cdot P(b^0) \cdot P(s(E)) = \\ \int dE\ G(E, E_i) \eta(E) e^{-B\delta t} S(t,E) \delta t e^{-S(t,E)\delta t} \simeq \\ \int dE\ G(E, E_i) \eta(E) \cdot S(t,E) \delta t + O(\delta t^2) \simeq \\ \delta t \int dE\ G(E, E_i) \cdot R(t,E) \end{array} \tag{A10}$$

In this expression, the probability that a signal (a positron) with energy E produces a datum with measured energy E_i, is decomposed as follows:

$$P(d(E_i) \mid s(E), b^0) = G(E, E_i) \cdot \eta(E) \tag{A11}$$

The new function G, defined when $\eta(E) \neq 0$, is called smearing. We assume that it is independent from the time when the positron is produced and from the time when the signal is detected. In order to understand the meaning of the smearing, we use the sum rule of probability, $P(A \mid B) + P(\overline{A} \mid B) = 1$, and obtain

$$\begin{array}{l} P(d^1 \mid s(E), b^0) + P(d^0 \mid s(E), b^0) = 1, \\ \int dE'\ P(d(E') \mid s(E), b^0) + (1 - \eta(E)) = 1, \\ \int dE'\ G(E, E') \cdot \eta(E) + 1 - \eta(E) = 1, \\ \eta(E) \cdot \int dE'\ G(E, E') = \eta(E) \end{array} \tag{A12}$$

The last equation implies that the function $G(E, E')$ is normalized to the unity

$$\int dE'\ G(E, E') = 1, \tag{A13}$$

The domain of integration includes all possible energies of the detected event. The last term that we must calculate is

$$\begin{array}{l} P(d(E_i), s^0, b^1) = \int dE\ P(d(E_i), s^0, b(E)) = \\ \int dE\ P(d(E_i), s^0 \mid b(E)) P(b(E)) = \\ \int dE\ P(d(E_i) \mid s^0, b(E)) P(b(E)) P(s^0) \equiv \\ \int dE\ \delta(E - E_i) \cdot \delta t B(E) \cdot e^{-B(E)\delta t} e^{-S(t)\delta t} \simeq \\ \int dE\ \delta(E - E_i) \cdot \delta t B(E) + O(\delta t^2) = \delta t B(E_i) \end{array} \tag{A14}$$

where we used our definition of background including the Dirac function $P(d(E_i) \mid s^0, b(E)) \equiv \delta(E - E_i)$, that implies among the other things that $P(d^1 | s^0, b(E)) = \delta t\ B(E)$. In this way we found

$$\begin{array}{l} P(d(E_i)) = P(d(E_i), s^0, b^1) + P(d(E_i), s^1, b^0) = \\ = \delta t B(E_i) + \delta t \int dE\ G(E, E_i) \cdot R(t,E). \end{array} \tag{A15}$$

3. Summary and remarks

Plugging Eqs. A8 and A15 in Eq. A1, then using the definition of the likelihood, we conclude

$$\begin{array}{l} \mathcal{L} = \prod_{i=1}^{N} P_i = \\ \prod_{j=1}^{N-N_d} e^{-[B+R(t_j)]\delta t} \cdot \\ \prod_{i=1}^{N_d} \delta E [\delta t B(E_i) + \delta t \int dE\ G(E, E_i) R(t_i, E)] \simeq \\ (\delta t \delta E)^{N_d} e^{-\int_T dt(B+R(t))} \cdot \\ \prod_{i=1}^{N_d} [B(E_i) + \int dE\ G(E, E_i) R(t_i, E)] \end{array} \tag{A16}$$

that is the expression of the likelihood, associated to the collected data set. We have neglected the difference between the integral taken over the *entire* duration of the data taking T, and the integral taken over the non-detection intervals; but this difference is negligible, provided that $\delta t \ll T$.

As a simple test of Eq. A16, consider the likelihood given in PDG [90] for the case of n observed events:

$$L \propto (n_b + \eta n_s)^n e^{-(n_b + \eta n_s)} \tag{A17}$$

where a finite and *constant* detection efficiency η is considered.[7] We know that there are on average n_b background events in a given observation time T and we want

[7] Ref. [90] assumes that the background and the signal are Poisson distributed. It is easy to show that if the number of *produced* positrons is distributed as a Poisson process, also the number of *detected* positrons, that is smaller by a factor η, is is distributed as a Poisson process (the inclusion of the efficiency can be thought of as the convolution with a Binomial).

to evaluate the number of signal events n_s. Thus we minimize the likelihood, imposing $\partial L/\partial n_s = 0$, and we find the obvious response:

$$n_s = \frac{n - n_b}{\eta} \tag{A18}$$

namely: the estimated number of signal events is given by the difference of the number of observed and of background events, increased by the factor $1/\eta > 1$ to take into account the imperfect detection efficiency. The likelihood in Eq. A17 derives from Eq. A16 as follows. Suppose that signal and background are uniformly distributed over the energy

$$B = \frac{n_b}{TE_*} \text{ and } S = \frac{n_s}{TE_*} \quad \text{if } 0 < E < E_* \tag{A19}$$

being zero elsewhere. Assume that the energy is precisely measured: $G(E) = \delta(E - E_i)$. Plugging in Eq. A16 the definition of $R = \eta S$ given in Eq. A6 we obtain the same likelihood given in Eq. A17 for n observed event. The conclusion is simply that, in a suitable limit, we recover expected results as Eq. A18 from the likelihood shown in Eq. A16.

Eq. A16 is the form of the likelihood to be used in each detector. It is occasionally called the 'unbinned' likelihood, since it can be used to analyze the data without introducing a binning. We note that the likelihood in Eq. A16 agrees with the one of Ref. [32], the likelihood adopted in the most recent analyses of SN1987A data [41, 42].

Appendix B: Accretion energy spectrum

We derive two equations used to describe the energy spectrum of accretion $\bar{\nu}_e$.

1. Derivation of Eq. 13

We assume that, during accretion, the antineutrino flux is mostly produced by the weak reaction $e^+ n \to \bar{\nu}_e p$. The rate of this reaction is given by:

$$\Gamma = N_n \int_{m_e}^{\infty} dE_{e^+} \; \frac{d\, n_{e^+}}{d\, E_{e^+}} \; \beta_e c \int dE_\nu \; \frac{d\, \sigma_{e^+ n}}{d\, E_\nu}, \tag{B1}$$

where N_n is the number of target neutrons, assumed to be at rest, and where β_e is the positron velocity in natural units. The second integral yields the cross section as a function of the positron energy E_{e^+}. The distribution of the positrons $d\, n_{e^+} = 2d^3 p_e/h^3/(1+\exp[(E_{e^+} - \mu_{e^+})/T_a])$ has a negligible chemical potential [14], thus

$$\frac{d\, n_{e^+}}{d\, E_{e^+}}(E_{e^+}) = \frac{8\pi\beta_e}{(hc)^3} \; g_{e^+}(E_{e^+}, T_a), \tag{B2}$$

where g_{e^+} is given by Eq. 14. The range of integration of E_ν in Eq. B1 can be easily found from the expression:

$$E_\nu = \frac{E_e + \delta_+}{1 + (E_e - p_e \cos\phi)/m_n}, \tag{B3}$$

where $\cos\phi = \hat{n}_e \cdot \hat{n}_\nu$ is the cosine of the angle between the directions of the positron and the antineutrino, $\cos\phi \in [-1, 1]$, and where $\delta_+ = (m_n^2 - m_p^2 + m_e^2)/(2m_n) = 1.293$ MeV $\approx \delta_-$ in Eq. 5. The dependence on the antineutrino energy E_ν is as follows:

$$\frac{d\,\Gamma}{dE_\nu} = \frac{8\pi c}{(hc)^3} N_n \int dE_{e^+} \; \beta_e^2 \; g_{e^+} \; \frac{d\,\sigma_{e^+ n}}{d\, E_\nu}. \tag{B4}$$

The cosine can take all values for fixed $E_\nu \geq E_{min}$, with

$$E_{min} = \frac{m_e + \delta_+}{1 + m_e/m_n} \approx 1.803 \text{ MeV}, \tag{B5}$$

[for smaller E_ν, only certain values of $\cos\phi$ around $\cos\phi = -1$ are allowed; but this happens in an interval of E_ν wide only about 1 eV]. The range for E_{e^+} is:

$$E_{e^+} = \frac{(E_\nu - \delta_+)(1-\epsilon) - \epsilon\cos\phi\sqrt{(E_\nu - \delta_+)^2 - m_e^2(1+\Delta)}}{1+\Delta}, \tag{B6}$$

where $\epsilon = E_\nu/m_n$ and $1 + \Delta = (1-\epsilon)^2 - \epsilon^2\cos\phi^2$. From this equation it is clear that the E_{e^+} range is pretty narrow for the energies $E_\nu \ll m_n$ in which we are interested; thus, we approximate the expression in Eq. B4 as:

$$\frac{d\,\Gamma}{d\,E_\nu} \approx \frac{8\pi c}{(hc)^3} N_n g_{e^+}(\bar{E}_{e^+}(E_\nu), T_a) \int dE_{e^+} \beta_e^2 \; \frac{d\,\sigma_{e^+ n}}{d\,E_\nu} \tag{B7}$$

where the positron distribution is calculated at the central point of the interval of cosine, namely at $\cos\phi = 0$:

$$\bar{E}_{e^+}(E_\nu) = \frac{E_\nu - \delta_+}{1 - E_\nu/m_n}. \tag{B8}$$

Eq. B7 gives the $\bar{\nu}_e$ flux in Eq. 13; the integral will be discussed a while. The advantage of Eq. B7 is that the dependence on the parameter T_a has been extracted from the integral. The integral can be calculated once forever and we are left with a simpler expression. We checked that, in the most relevant range $T_a = 1 - 4$ MeV, the approximated expression agrees with the correct one at the 1% level for energies $E_\nu < 10\, T_a$, and even better when $d\Gamma/dE_\nu$ is integrated in E_ν: indeed, the rate Γ is precise at 0.1%.

2. Derivation of Eq. 15

The cross section in Eq. 15, precisely defined as a numerical approximation of the integral in Eq. B7, was obtained adapting the calculation of [57] for the inverse beta decay reaction. In fact, the differential cross section

$$\frac{d\,\sigma_{e^+ n}}{d\,E_\nu}(E_{e^+}, E_\nu) = \frac{G_F^2 \; \cos^2\theta_C}{256\pi \; m_n \; p_e^2} |\mathcal{M}|^2 (1 + r) \tag{B9}$$

has the *same* matrix element $|\mathcal{M}|^2(s-u,t)$. What changes is the expression of the invariants, now given by: $s-u=2m_n(E_\nu+E_e)+m_e^2$ and $t=m_p^2-m_n^2+2m_n(E_\nu-E_e)$. The factor $r(E_e)$ describes the small QED radiative corrections; we use expression in [57]. The constant in front to the differential cross section is 2 times smaller than the one for inverse beta decay, because the antineutrino has 1 helicity state whereas the positron has 2. The characteristic $1/\beta_e$ behavior of an exothermic reaction (such as $e^+n\rightarrow\bar{\nu}_e p$) is compensated by the 2 explicit factors β_e from the positron phase space and from the relative velocity between e^+ and n in the reaction rate, included in σ_{e^+n}.

Our cross section compares well with the approximation of Tubbs and Schramm [91, 92]:

$$\sigma_{e^+n}^{TS}=1.7\times10^{-44}\frac{1+3g_A^2}{8}\left(\frac{E_\nu}{m_e}\right)^2, \qquad \text{(B10)}$$

with $g_A=-1.27$, since the percentage deviation $100(1-\sigma_{e^+n}^{TS}/\sigma_{e^+n})$ at $E_\nu=5,10,20,30$ MeV is just -1%, -2%, -6%, -11% (or -1%, -3%, -7%, -10% when comparing with the approximation of σ_{e^+n} in Eq. 15).

The cross section used in [35] is formally less correct, since it is the same as the above approximation but replacing $g_A^2\rightarrow|g_A|\approx1.254$. [This is stated in Eq. (4.5) of LL and can be checked by the value of the energy radiated during accretion, their Eq. (6.2)]. The deviation $100(1-\sigma_{e^+n}^{LL}/\sigma_{e^+n})$ is not large; for $E_\nu=5,10,20,30$ MeV is 17%, 16%, 13%, 10% (or 18%, 16%, 13%, 10% when comparing with Eq. 15).

Our parametrization of $\bar{\nu}_e$ spectrum, Eq. 14, differs also for another reason with the one of LL, since we adopt the positron flux calculated in $E_e(E_\nu)$ (defined in Eq. B8), whereas LL use the antineutrino flux calculated in E_ν, namely, $g\rightarrow E_\nu^2/[1+\exp(E_\nu/T_a)]$. Also this modification acts in the direction of increasing the expected flux. The difference can be quantified by evaluating these integral of the fluxes $\Phi_{\bar{\nu}_e}(T_a)=\int\frac{d\Phi_{\bar{\nu}_e}}{dE_\nu}\,dE_\nu$: indeed, $1-\Phi_{\bar{\nu}_e}^{LL}(T_a)/\Phi_{\bar{\nu}_e}(T_a)=54\%$, 35%, 26% or 19% for $T_a=1$, 2, 3 or 4 MeV; namely, our flux is significantly larger.

[1] H. T. Janka, A. Marek, B. Mueller and L. Scheck, arXiv:0712.3070 [astro-ph].
[2] S.E. Woosley and T.A. Weaver, Astrophys. J. Suppl. **101**(1995)181.
[3] K. Nomoto *et al.*, Nucl. Phys. A, **777** (2006), 424-458.
[4] H. T. Janka, R. Buras and M. Rampp, Nucl. Phys. A **718** (2003) 269.
[5] A. Burrows, J. Hayes and B. A. Fryxell, Astrophys. J. **450** (1995) 830 [arXiv:astro-ph/9506061].
[6] C. L. Fryer and K. C. B. New, Living Rev. Rel. **6** (2003) 2.
[7] K. Kotake, K. Sato and K. Takahashi, Rept. Prog. Phys. **69** (2006) 971 [arXiv:astro-ph/0509456].
[8] S. A. Colgate and R. H. White, Astrophys. J. **143** (1966) 626.
[9] A. Burrows, Astrophys. J. **334** (1988) 891.
[10] H. A. Bethe and J. R. Wilson, Astrophys. J. **295** (1985) 14.
[11] D. K. Nadyozhin, Astrophys. Space Sci. **53** (1978) 131.
[12] H. T. Janka, A. Marek and F. S. Kitaura, AIP Conf. Proc. **937** (2007) 144 [arXiv:0706.3056 [astro-ph]].
[13] A. Marek and H. Th. Janka, astro-ph:0708.3372v1.
[14] H.Th. Janka, A&A, 368 (2001) 527.
[15] R. M. Bionta *et al.* [IMB Collaboration], Phys. Rev. Lett. **58** (1987) 1494.
[16] C. B. Bratton *et al.* [IMB Collaboration], Phys. Rev. D **37** (1988) 3361.
[17] K. Hirata *et al* [Kamiokande-II Collaboration], Phys. Rev. Lett. **58** (1987) 1490.
[18] K. S. Hirata *et al.* [Kamiokande-II Collaboration], Phys. Rev. D **38** (1988) 448.
[19] E.N. Alekseev, L.N. Alekseeva, I.V. Krivosheina and V.I. Volchenko, Phys.Lett.B **205** (1988) 209.
[20] A. E. Chudakov, Y. S. Elensky and S. P. Mikheev, JETP Lett. **46** (1987) 373 [Pisma Zh. Eksp. Teor. Fiz. **46** (1987) 297].
[21] S. W. Bruenn, Phys. Rev. Lett. **59** (1987) 938; S. H. Kahana, J. Cooperstein and E. Baron, Phys. Lett. B **196** (1987) 259.
[22] J. N. Bahcall, A. Dar and T. Piran, Nature **326** (1987) 135; D. N. Spergel, T. Piran, A. Loeb, J. Goodman and J. N. Bahcall, Science **237** (1987) 1471; J. N. Bahcall, T. Piran, W. H. Press and D. N. Spergel, Nature **327** (1987) 682.
[23] K. Sato and H. Suzuki, Phys. Rev. Lett. **58**, 2722 (1987); Phys. Lett. B **196** (1987) 267; Prog. Theor. Phys. **79** (1988) 725.
[24] J. Arafune and M. Fukugita, Phys. Rev. Lett. **59** (1987) 367; J. Arafune, M. Fukugita, T. Yanagida and M. Yoshimura, Phys. Lett. B **194** (1987) 477.
[25] P.O. Lagage, M. Cribier, J. Rich and D. Vignaud, Phys.Lett.B **193** (1987) 127; L. Wolfenstein, Phys.Lett.B **194** (1987) 197; D. Notzold, Phys.Lett.B **196**, 315 (1987); H. Minakata and H. Nunokawa, Phys.Rev.D **38** (1988) 3605.
[26] See J. N. Bahcall, chap. 15 of *Neutrino astrophysics,* Cambridge University Press, 1989 and references therein for a summary of several early analyses.
[27] V. L. Dadykin, G. T. Zatsepin and O. G. Ryazhskaya, Sov. Phys. Usp. **32** (1989) 459.
[28] H.-T. Janka and W. Hillebrandt, A& A **224** (1989) 49.
[29] J. M. Lattimer, A. Yahil, Astrophys. J. 340 (1989) 426.
[30] A.Y. Smirnov, D.N. Spergel and J.N. Bahcall, Phys. Rev. D **49** (1994) 1389 [arXiv:hep-ph/9305204].
[31] P. J. Kernan and L. M. Krauss, Nucl. Phys. B **437** (1995) 243 [arXiv:astro-ph/9410010].
[32] B. Jegerlehner, F. Neubig and G. Raffelt, Phys. Rev. D **54** (1996) 1194 [arXiv:astro-ph/9601111].
[33] A. Malgin, Nuovo Cim. C **21** (1998) 317.
[34] C. Lunardini and A. Y. Smirnov, Phys. Rev. D **63** (2001)

073009 [arXiv:hep-ph/0009356].
[35] T. J. Loredo and D. Q. Lamb, Phys. Rev. D **65** (2002) 063002.
[36] M. Kachelriess, A. Strumia, R. Tomas and J. W. F. Valle, Phys. Rev. D **65** (2002) 073016 [arXiv:hep-ph/0108100].
[37] H. Minakata and H. Nunokawa, Phys. Lett. B **504** (2001) 301 [arXiv:hep-ph/0010240].
[38] V. Barger, D. Marfatia and B. P. Wood, Phys. Lett. B **532** (2002) 19 [arXiv:hep-ph/0202158].
[39] C. Lunardini and A. Y. Smirnov, Astropart. Phys. **21** (2004) 703 [arXiv:hep-ph/0402128].
[40] M. L. Costantini, A. Ianni and F. Vissani, Phys. Rev. D **70**, 043006 (2004) [arXiv:astro-ph/0403436].
[41] A. Mirizzi and G. G. Raffelt, Phys. Rev. D **72**(2005) 063001.
[42] C. Lunardini, Astropart. Phys. **26** (2006) 190 [arXiv:astro-ph/0509233].
[43] M. L. Costantini, A. Ianni, G. Pagliaroli and F. Vissani, JCAP **05** (2007) 014.
[44] P. Antonioli *et al.*, New J. Phys. **6** (2004) 114 [arXiv:astro-ph/0406214].
[45] L. Wolfenstein, Phys. Rev. D **17** (1978) 2369.
[46] S. P. Mikheev and A. Y. Smirnov, Sov. J. Nucl. Phys. **42** (1985) 913 [Yad. Fiz. **42** (1985) 1441].
[47] S. P. Mikheev and A. Y. Smirnov, Sov. Phys. Usp. **29** (1986) 1155.
[48] T. K. Kuo and J. T. Pantaleone, Rev. Mod. Phys. **61** (1989) 937.
[49] HOMESTAKE Collaboration, Astrophs. J. 496 (1998) 505; Kamiokande Collaboration, Phys. Rev. Lett. 77 (1996) 1683; GALLEX Collaboration, Phys. Lett. B447 (1999) 127; SAGE Collaboration, Phys. Rev. C60 (1999) 055801.
[50] Y. Fukuda *et al.* [Super-Kamiokande Collaboration], Phys. Rev. Lett. **81** (1998) 1562 [arXiv:hep-ex/9807003].
[51] M. Ambrosio *et al.* [MACRO Collaboration], Phys. Lett. B **434** (1998) 451 [arXiv:hep-ex/9807005].
[52] W. W. M. Allison *et al.* [Soudan-2 Collaboration], Phys. Lett. B **449** (1999) 137 [arXiv:hep-ex/9901024].
[53] Q. R. Ahmad *et al.* [SNO Collaboration], Phys. Rev. Lett. **89** (2002) 011301 [arXiv:nucl-ex/0204008].
[54] K. Eguchi *et al.* [KamLAND Collaboration], Phys. Rev. Lett. **90** (2003) 021802 [arXiv:hep-ex/0212021].
[55] E. Aliu *et al.* [K2K Collaboration], Phys. Rev. Lett. **94** (2005) 081802 [arXiv:hep-ex/0411038].
[56] D. G. Michael *et al.* [MINOS Collaboration], Phys. Rev. Lett. **97** (2006) 191801 [arXiv:hep-ex/0607088].
[57] A. Strumia and F. Vissani, Phys. Lett. B **564** (2003) 42.
[58] V. L. Dadykin *et al.*, JETP Lett. **45** (1987) 593 [Pisma Zh. Eksp. Teor. Fiz. **45** (1987) 464]; M. Aglietta *et al.*, Europhys. Lett. **3** (1987) 1315.
[59] A. De Rujula, Phys. Lett. B **193** (1987) 514; V.S. Berezinsky, C. Castagnoli, V.I. Dokuchaev, P. Galeotti, Nuovo Cim. C11 (1988) 287.
[60] V. S. Imshennik and O. G. Ryazhskaya, Astron. Lett. **30** (2004) 14 [arXiv:astro-ph/0401613].
[61] A. Drago, G. Pagliara, G. Pagliaroli, F. L. Villante and F. Vissani, AIP Conf. Proc. **1056** (2008) 256 [arXiv:0809.0518 [astro-ph]].
[62] F. Vissani and G. Pagliaroli, arXiv:0807.1301 [astro-ph], presented at the 4th NO-VE International Workshop (2008) edited by Milla Baldo-Ceolin, pages 215-231.
[63] G. Pagliaroli, M. L. Costantini and F. Vissani, arXiv:0804.4598 [astro-ph], in proceedings of IFAE 2007, ed. by G. Carlino, G. D'Ambrosio, L. Merola, P. Paolucci, G. Ricciardi, page 225.
[64] A.S. Dighe and A.Yu. Smirnov, Phys. Rev. D **62** (2000) 033007
[65] M.L. Costantini, PhD thesis, L'Aquila University, 2007, Sect. 1.2. PDF file available at `http://www.infn.it/thesis/thesis_dettaglio.php?tid=1794`.
[66] D. K. Nadyozhin and V. S. Imshennik, Int. J. Mod. Phys. A **20** (2005) 6597 [arXiv:astro-ph/0501002].
[67] D. K. Nadyozhin and I. V. Ostroshchenko, Astron. Zh. **57** (1980) 78.
[68] M.T. Keil, G.G. Raffelt and H.T. Janka, Astrophys. J. **590** (2003) 971.
[69] G.L. Fogli, E. Lisi, D. Montanino and A. Palazzo, Phys. Rev. D **65** (2002) 073008
[70] J. T. Pantaleone, Phys. Lett. B **287** (1992) 128.
[71] G. Sigl and G. Raffelt, Nucl.Phys.B **406** (1993) 423.
[72] J. T. Pantaleone, Phys. Lett. B **342** (1995) 250 [arXiv:astro-ph/9405008].
[73] Y. Z. Qian and G. M. Fuller, Phys. Rev. D **51** (1995) 1479 [arXiv:astro-ph/9406073].
[74] H. Duan, G. M. Fuller, J. Carlson and Y. Z. Qian, astro-ph/0703776.
[75] V. A. Kostelecky and S. Samuel, Phys. Lett. B **318** (1993) 127.
[76] H. Duan, G. M. Fuller and Y. Z. Qian, Phys. Rev. D **74** (2006) 123004 [arXiv:astro-ph/0511275].
[77] G. G. Raffelt and A. Y. Smirnov, Phys. Rev. D **76** (2007) 081301 [Erratum-ibid. D **77** (2008) 029903] [arXiv:0705.1830 [hep-ph]].
[78] H. Duan, G. M. Fuller, J. Carlson and Y. Q. Zhong, Phys. Rev. Lett. **99** (2007) 241802 [arXiv:0707.0290 [astro-ph]].
[79] G.L. Fogli, E. Lisi, A. Marrone, A. Mirizzi, JCAP 12 (2007) 010 [arXiv:0707.1998v2 [hep-ph]].
[80] B. Dasgupta, A. Dighe, A. Mirizzi, [arXiv:0802.1481v2 [hep-ph]].
[81] G. Pagliaroli, M. L. Costantini, A. Ianni and F. Vissani, arXiv:0705.4032 [astro-ph].
[82] A. Strumia and F. Vissani, arXiv:hep-ph/0606054, a review regularly updated on the web.
[83] A. Esteban-Pretel, S. Pastor, R. Tomas, G.G. Raffelt, G. Sigl, Phys. Rev. D 77 (2008) 065024 [arXiv:0712.1137 [astro-ph]].
[84] A. Esteban-Pretel, A. Mirizzi, S. Pastor, R. Tomas, G.G. Raffelt, P.D. Serpico, G. Sigl, [arXiv:0807.0659v1 [astro-ph]].
[85] F. Cavanna, M.L. Costantini, O. Palamara, F. Vissani, Surveys HEP **19** (2004) 35.
[86] As in Fig.A1 of N.Y. Agafonova *et al.*, Astropart. Phys. **27** (2007) 254.
[87] G. L. Fogli, E. Lisi, A. Marrone, A. Palazzo and A. M. Rotunno, Phys. Rev. Lett. **101** (2008) 141801 [arXiv:0806.2649 [hep-ph]].
[88] G. Pagliaroli and F. Vissani, arXiv:0810.0456 [astro-ph], accepted for publication in Astronomy Letters.
[89] G. Cowan, *Statistical Data Analysis*, Oxford Science Publications 1998.
[90] C. Amsler et al., [PDG Collaboration], Phys. Lett. B667, 1 (2008), Sect.32 on Statistics, Eq. (32.33).
[91] D. L. Tubbs and D. N. Schramm, Astrophys. J. **201** (1975) 467.
[92] H.-T. Janka, R. Moenchmeyer, A&A 209 (1989) L5.